n-p Triple-Scattering Parameter D_t at 197 MeV*

D. SPALDING,† A. R. THOMAS, AND E. H. THORNDIKE
Department of Physics and Astronomy, University of Rochester, Rochester, New York
(Received 9 February 1967)

The n-p triple-scattering parameter D_t has been measured at 197 MeV at three angles. The measurements were made by bombarding a liquid-deuterium target with polarized protons, and spin-analyzing high-energy neutrons recoiling into forward angles. Spin analysis was accomplished by a charge-exchange scattering on CH_2. The measurements are related to the D_t parameter for free n-p scattering through an impulse-approximation calculation which includes the s-wave final-state interaction between the incident proton and the proton in the deuteron. Values obtained for the free np D_t parameter are: $+0.095\pm0.068$, -0.014 ± 0.071, and $+0.058\pm0.103$ at free n-p center-of-mass scattering angles of 147.4°, 138.6°, and 126.9°, respectively. These values are compared with the phase-shift solutions YLAN of Breit and collaborators, and the energy-independent solution of Arndt and MacGregor. Solutions YLAN 0, 1, 2, 2M, 3, and the Arndt-MacGregor solution do *not* agree with the data. Solutions YLAN 3M and 4M fit the data quite well.

I. INTRODUCTION

WE have measured[1] the n-p triple-scattering parameter D_t by bombarding a liquid-deuterium target with 197-MeV polarized protons from the University of Rochester 130-in. Synchrocyclotron and spin-analyzing neutrons recoiling at laboratory angles of 15°, 20°, and 25°. Spin analysis was accomplished by a charge exchange scattering on CH_2. The measurements are related to free n-p scattering using an impulse approximation calculation described in an earlier paper.[2]

The sub-t triple-scattering parameters differ from the conventional ones in that the recoiling target particle rather than the incident particle is detected. D_t is defined by

$$\langle\boldsymbol{\sigma}_b\rangle_f\cdot\mathbf{n}_t=(P_t+D_t\langle\boldsymbol{\sigma}_a\rangle_i\cdot\mathbf{n}_t)/(1+P_t\langle\boldsymbol{\sigma}_a\rangle_i\cdot\mathbf{n}_t). \quad (1)$$

Here a denotes the incident particle, and b the target particle; $\langle\boldsymbol{\sigma}_b\rangle_f$ is the final polarization of the target particle, and $\langle\boldsymbol{\sigma}_a\rangle_i$ is the initial polarization of the incident particle. The $\mathbf{n}_t$ is defined by

$$\mathbf{n}_t=(\mathbf{k}\times\mathbf{k}_t)/|\mathbf{k}\times\mathbf{k}_t|, \quad (2)$$

where $\mathbf{k}$, $\mathbf{k}_t$ are unit vectors in the momentum direction of particle a before scattering and particle b after scattering, respectively. P_t is the sub-t polarization parameter defined by

$$I=I_0(1+P_t\langle\boldsymbol{\sigma}_a\rangle_i\cdot\mathbf{n}_t). \quad (3)$$

I is the cross section due to a polarized incident beam, and I_0 is that due to an unpolarized beam.

The following section describes the experimental apparatus and procedures, while Secs. III and IV describe the data analysis and results.

II. APPARATUS AND PROCEDURE

The experimental layout is shown in Fig. 1. Primary components are the beam, target, and spin analyzers.

The Beam

The internal synchrocyclotron beam was stochastically accelerated[3] onto a carbon target, producing a 90% polarized proton beam with a 30% duty cycle. The beam energy spectrum consisted of a symmetric peak and a low-energy tail. The peak, centered at 205 MeV, had a full width at half-maximum of 11 MeV. The low-energy tail extended down to 135 MeV, and contained $\frac{1}{4}$ the intensity of the peak. Allowing for target thickness and detection efficiency, this leads to an effective mean energy at scattering of 197 ± 2 MeV and an rms spread of ±11 MeV. During transport, the beam polarization was rotated into a horizontal plane by means of the solenoid magnet shown in Fig. 1. The sign of the beam polarization could be changed by reversing the current direction through the solenoid. (The two possibilities, "normal" and "reverse," are designated N and R.) During the experiment the beam position was determined frequently with particular attention being paid to any beam motion caused by reversing the solenoid current. Beam intensity was monitored with an air-filled ion chamber.

The Target

The liquid deuterium cup was a horizontal cylinder 5 in. long×5 in. in diameter with 0.003-in. Be-Cu walls. Its orientation transverse to the proton beam is shown in Fig. 1.

The Spin Analyzers

The spin of neutrons recoiling from the deuterium target was analyzed with two identical analyzers I and II placed symmetrically above and below the beam. The second scattering angle θ_2 was adjustable, but the

* Work supported by the U. S. Atomic Energy Commission. Based on a portion of a thesis submitted by D. Spalding in partial fulfillment of the requirements for the Ph.D. degree in Physics at the University of Rochester, Rochester, N. Y.

† Present address: Sarah Mellon Scaife Radiation Laboratory, University of Pittsburgh, Pittsburgh, Pennsylvania.

[1] This work is contained in D. Spalding, thesis, University of Rochester, 1966 (unpublished). Copies available on request.

[2] N. W. Reay, E. H. Thorndike, D. Spalding, and A. R. Thomas, Phys. Rev. **150**, 801 (1966).

[3] E. Nordberg, IEEE Trans. Nucl. Sci. **NS12**, 973 (1965).

third scattering angle θ_3 was designed to be fixed at 25°. An examination of Fig. 1 shows that for any event detected, both the second and third scattering planes are nearly vertical and parallel to the proton beam line, making the normals to the second and third scattering planes nearly parallel (or antiparallel) to each other. To be detected, a neutron from the deuterium target has to pass through the veto counters $\bar{1}$ and $\bar{2}$ and convert in the converter (C), a 5-in.×12-in.×2-in. block of polyethylene. The conversion proton is counted in a recoil telescope 3456, having passed through a variable copper range requirement placed between counters 5 and 6. The counters were all Pilot B scintillon viewed by RCA 6810A photomultipliers. Computed detection efficiency versus energy of the detected neutron is shown in Fig. 2. The rms spread in θ_2 is ±2.0°, 2.0°, and 2.6° at θ_2 of 15°, 20°, and 25°, respectively. At second scattering angles where the proton beam would strike some of the counters in the analyzers, a lead beam stopper was used, as shown in Fig. 1. Not shown is a helium bag placed between the target and the lead beam stopper, to reduce air scattering of the proton beam into the analyzers. Also omitted is the beam-scanning counter placed immediately downstream of the ion chamber.

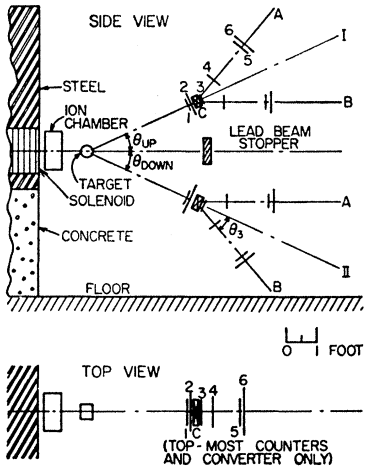

FIG. 1. Experimental layout. Counters 1 and 2 are veto counters, and 3, 4, 5, and 6 are yes counters arranged to detect conversion protons which come from the polyethylene block C and move along lines IA, IB, IIA, and IIB. The lead beam stopper prevents the direct beam from striking the counters 4, 5, and 6. Not shown is a polyethylene helium bag placed between the target and beam stopper to reduce air scattering of the direct beam into the counters.

Electronics

The phototube pulses from the analyzers I and II were processed by two similar electronic arrangements set up to scale $\bar{1}\bar{2}3456$ counts. All active components except the scalers were Chronetics modules.

Procedures

All data were taken during one cyclotron run. At the beginning of the run a differential range curve of the incident proton beam was measured. After correction for nuclear absorption, the curve and the data of Rich and Madey[4] were used to find the beam energy and intensity distribution information quoted above. No beam polarization measurement was made; the value quoted in Ref. 2 was used. At each angle, conversion proton integral range curves were taken by observing the rate $\bar{1}\bar{2}3456$ as a function of copper-range requirement in the polarimeter for converter in, and target full and empty. These neutron range curves were used to determine the absorber threshold used in the measurement of asymmetry. Also at each angle, mechanical measurements were made to check the value of second and third scattering angles.

The asymmetry data were taken in "sets," one of which took approximately 4 h to complete. Target full and target empty data at a given θ_2 were taken consecutively, with the solenoid reversed many times at each θ_2 and at each target condition. As a check, at some angles asymmetries were remeasured at a proton beam intensity one-half of the normal, and at all angles they were remeasured at a range requirement different from normal. As a check on the electronic arrangement, at θ_2 of 25°, the measurement at one absorber setting (0.30-in. Cu) was done twice. The second time was with "modified" electronics where open stubs used to lengthen the $\bar{1}$ and $\bar{2}$ pulses were removed and compensated for by increasing the pulse-length setting on $\bar{1}$ and $\bar{2}$ discriminators.

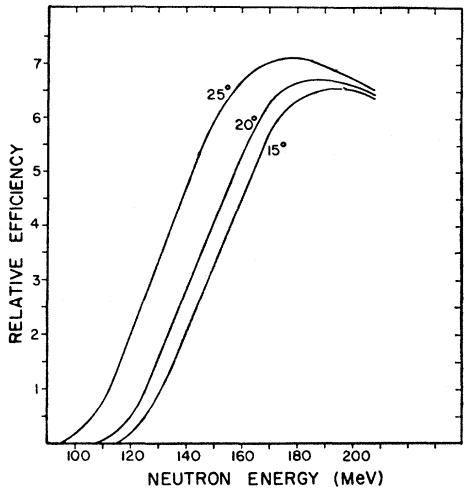

FIG. 2. Calculated relative efficiency versus incident neutron energy. The curves are for absorber settings of 0.45 in., 0.40 in., and 0.30 in. of copper at θ_2 of 15°, 20°, and 25°, respectively. The data used in Sec. IV to arrive at the final values of D_t were taken at these absorber settings, with the exception of that at 25°, where one third of the data were taken at 0.20 in. rather than 0.30 in.

[4] M. Rich and R. Madey, University of California Radiation Laboratory Report No. UCRL-2301 (unpublished).

TABLE I. Uncombined values of D_t and their errors.

Nom. θ_2 (lab)	Copper absorber (in.)	Relative beam intensity	$D_{t\mathrm{I}}$	$D_{t\mathrm{II}}$
15°	0.45	1.0	−0.003±0.084	+0.147±0.088
	0.45	0.5	+0.062 0.079	+0.147±0.082
	0.65	1.0	+0.101 0.130	+0.176 0.133
20°	0.40	1.0	−0.082±0.080	−0.027±0.078
	0.40	0.5	+0.013 0.104	+0.085 0.107
	0.60	1.0	+0.045 0.102	+0.155 0.112
25°	0.20	1.0	+0.059±0.169	+0.069±0.161
	0.30	1.0	−0.072 0.160	+0.244 0.178
	0.45	1.0	−0.190 0.190	−0.188 0.179
	0.30[a]	1.0	+0.116 0.147	−0.011 0.133

[a] Using modified veto electronics.

Random counts of the variety $(\bar{1}\bar{2}3):(456)$ were taken simultaneously with the neutron data, while the only other random of importance, $(\bar{1}\bar{2}34):(56)$, was periodically recorded between sets of neutron data. Target out neutron counts were typically 20% of target in minus target out, while all randoms together contributed ∼1% of target in counts.

Certain checks were made periodically: vertical beam profiles were made to measure solenoid associated beam motion, $1\bar{2}3456$ and 13456 rates were taken to check $\bar{2}$ efficiency, and 3456 rates were measured as an additional monitor.

III. DATA ANALYSIS

Formula for D_t

For each 456 telescope (i.e., IA, IB, IIA, or IIB) one may define an asymmetry:

$$\epsilon=\frac{N-R}{N+R}. \tag{4}$$

N, R are the fully subtracted $\bar{1}\bar{2}3456$ rates with solenoid N or R. Define the intermediate quantities:

$$q=[P_3P_t(\mathbf{n}_t\cdot\mathbf{n}_3)]_{\mathrm{av}}, \tag{5}$$

$$F_{\mathrm{I}}=(1+q)\epsilon_{\mathrm{IA}}-(1-q)\epsilon_{\mathrm{IB}}, \tag{6a}$$

$$F_{\mathrm{II}}=(1-q)\epsilon_{\mathrm{IIA}}-(1+q)\epsilon_{\mathrm{IIB}}. \tag{6b}$$

Here P_3 and $\mathbf{n}_3$ are respectively the analyzing power and normal to the scattering plane for the third scattering. The average is weighted by cross section, and is computed over the nonzero size of the parts of the analyzers. One may now write[5]

$$D_t=\frac{\frac{1}{2}(F+c_1+c_2)}{[P_3\langle\sigma_a\rangle_{iy}n_{ty}(\mathbf{n}_t\cdot\mathbf{n}_3)]_{\mathrm{av}}}. \tag{7}$$

F is either F_{I} or F_{II}. The y direction is horizontal and transverse to the proton beam, and $\mathbf{n}_t$, $\mathbf{n}_3$, P_3, and the average are the same as for Eq. (5). c_1 corrects F for solenoid associated beam motion and veto counter inefficiency. It was typically 15% of F. c_2 corrects F for effects associated with the nonzero size of the parts of the spin analyzer. Specifically, the finite length of the CH_2 converter allowed $\mathbf{n}_t$ and $\mathbf{n}_3$, to change from their nominal direction in a correlated fashion, mixing in R_t. Although c_2 was sometimes as much as 50% of F, it affected D_t by ∼+0.02.

Equation (7) appears elaborate at first glance. However, we note that $P_3\approx P_t\sim 0.1$, so that $q\sim 0.01$ and F is essentially a difference of asymmetries. Also, if all scatterings were with ideal geometry, the denominator of (7) would simply be $P_3\langle\sigma_a\rangle_{iy}$. Hence, (7) merely states that D_t is an average of a corrected difference of asymmetries renormalized by the product of beam polarization and third scattering analyzing power. P_3 has been obtained from the empirical expression

$$P_3=+0.130+1.5\times10^{-3}(\theta_2-25°)+1.2\times10^{-3}[E(n)-210\ \mathrm{MeV}].$$

This expression is a reasonable fit to free np polariza-

TABLE II. Average systematic differences. "I-II" difference: The difference between a value of D_t at a given beam intensity and absorber setting for analyzer I, and the corresponding analyzer II value at the same beam and absorber setting. The average is over all ten possible pairs of the values listed in Table I. "Intensity" difference: The difference between the high- and low-beam intensity values of D_t for a given analyzer and angle at range settings of 0.45 in., 0.40 in. at 15° and 20°, respectively. The average is over four pairs of values, and there were no applicable pairs at 25°. "Absorber" difference: The difference between the highest and lowest copper-range setting value of D_t for a given analyzer and angle. The average is over the six applicable pairs of values. "Electronics" difference: The difference between the averages over both analyzers of the two 0.30 in. Cu measurements at 25°, one measurement with normal electronics and one with the modified electronics.

Kind of difference	Average difference	No. standard deviations
I-II	−0.077±0.058	1.33
Intensity	−0.069±0.062	1.11
Absorber	−0.009±0.075	0.12
Electronics	+0.034±0.153	0.22

TABLE III. Internal consistency of D_t at each second scattering angle. Listed for D_t is the value of χ^2 resulting from a fit of all the data at a given angle by their average. Also shown is the probability P that each χ^2 value would occur, assuming the sole error in each measurement was the random error assigned in Table I. (This means there are assumed to be no unknown systematic differences in the data.)

Nominal θ_2	χ^2	P
15°	2.78	73%
20°	4.15	53%
25°	5.10	66%

[5] For a more detailed derivation, see Appendix III and Chap. III, Sec. C of Ref. 1.

tions[6] and phase-shift fits to them.[7] In particular, data[8] near 200 MeV and 25° lab are well fitted. $E(n)$ is the computed average energy of the neutrons. Values were 181, 166, and 151 MeV, corresponding to absorber settings of 0.45 in., 0.40 in., and 0.30 in. at θ_2 of 15°, 20°, and 25°, respectively. This energy information and the alignment checks mentioned in Sec. II have been used to find the analyzing power. The relative error in P_3 was roughly 30%, while that of the numerator of Eq. (7) was 60% or more. Hence, the uncertainty in P_3 is unimportant.

Internal Consistency

Table I lists the D_t values obtained under the various conditions imposed during the experiment.[9] An examination of that table shows that of all ten I-II pairs of corresponding values of D_t, nine have an analyzer II value more positive than that of analyzer I. If this distribution were random, this would be expected to happen once in roughly fifty identical experiments, suggesting a systematic difference between the two analyzers.

TABLE IV. Final values of D_t and its errors. The D_t values are a weighted average of the data at each angle. The error in the final D_t is the sum in quadrature of the one "random" and three "systematic" errors σ_r, σ_a, σ_b, and σ_c, which are also tabulated. The actual second-scattering angles used are shown along with their rms. spreads. These are an average over the two analyzers, which differed slightly.

θ_2(lab) ±rms spread	$\bar{D}_t$	σ_r	σ_a	σ_b	σ_c
15.5°±2.0°	+0.087±0.068	0.041	0.041	0.033	0.015
19.7°±2.0°	−0.018±0.071	0.045	0.041	0.033	0.016
25.3°±2.6°	+0.058±0.103	0.064	0.041	0.066	0.023

This and three other possible systematic errors are investigated in Table II, which lists average differences between D_t measurements; these should be consistent with zero if there were no systematic dependence of the D_t measurements on analyzer, beam intensity, copper range requirement, or veto counter set-up. An inspection of the table shows in fact that all average differences are within one and one-half standard deviations of zero. Any systematic effects of the kinds listed are thus obscured by the random errors in the data. This conclusion is further supported by the information in Table III where we find the data at each θ_2 are well fitted by their average. This would only be true if all systematic differences among the data were small compared to a typical random error. Again, we conclude that even if there are systematic errors in D_t, for which there is some evidence, it is reasonable to assume these errors are smaller than the random error in any given measurement. In this sense, then, the D_t data are found to have no internal inconsistencies.

TABLE V. D_t^{np} and the quantities by which it was obtained from D_t^{pd}. The correction $\Delta D_t = D_t^{np} - D_t^{pd}$ was calculated using the Yale phase shifts YLAN-3M; however, solutions 4M and A-M gave values that differed by less than 0.0075.

$\theta_{2\,\mathrm{lab}}$	$\theta_{2\,\mathrm{c.m.}}$	$aI_0^{np}/2bI_0^s$	ΔD_t	D_t^{np}
15.5°	147.4°	2.56	+0.008	+0.095±0.068
19.7°	138.6°	5.25	+0.004	−0.014±0.071
25.3°	126.9°	∞	+0.000	+0.058±0.103

Final Values of D_t

To obtain a final D_t at each θ_2, we take a weighted average of the form:

$$\bar{D}_t = \sum(D_t/\sigma^2)/\sum(1/\sigma^2), \tag{8}$$

where σ is the random error in the individual D_t measurements, and the sum is over all data except those taken at the highest absorber settings. These high absorber data were taken to demonstrate insensitivity on absorber of other data taken at still lower settings. They include only part of the neutron spectrum produced by the deuterium target and for this reason they are excluded.

The random error σ_r in $\bar{D}_t$ was obtained from the random errors in the individual D_t measurements. (Had this error instead been taken from the fluctuation of the data points about their mean, a slightly smaller value would have been obtained.)

Three sorts of systematic errors have been included. There is some evidence for systematic errors involving the choice of analyzer (I versus II), and the beam intensity. The errors σ_a and σ_b allow for these. The former is one half the weighted average of the I-II difference in D_t. The latter is, at 15° and 20°, one-half the weighted average of the difference between high-

TABLE VI. χ^2 from the comparison of experimental D_t with phase-shift predictions. Shown is the χ^2 from the comparison of the three data of this experiment and the value near 0° from Ref. 2 with predictions for inelastic pd scattering using the np to singlet ratios of Table V and the free np phase-shift sets listed below. P is the probability for four degrees of freedom that χ^2 would be the given value or greater. All solutions are ruled out except 3M, 4M, and A-M; A-M is strongly disfavored.

Phase-shift set	χ^2	P
2M	97	
2	88	
0	88	
1	36	
3	23	≪1%
A-M	11.2	3%
4M	3.9	43%
3M	1.5	82%

[6] R. Wilson, *The Nucleon-Nucleon Interaction* (John Wiley & Sons, Inc., New York, 1963).
[7] M. Hull, K. Lassila, H. Ruppel, F. McDonald, and G. Breit, Phys. Rev. **122**, 1606 (1961).
[8] D. Spalding, A. R. Thomas, N. W. Reay, and E. H. Thorndike, Phys. Rev. **150**, 806 (1966).
[9] For a more elaborate discussion, see Ref. 1, Chap. III, Sec. D.

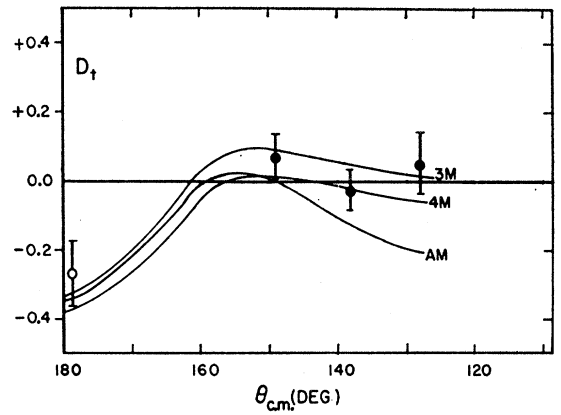

FIG. 3. Final D_t values for p-d scattering compared with the most favored phase shift predictions. The abscissa is the equivalent free n-p center of mass scattering angle. The filled circles are the data from this experiment, and the open circle near 180° is R_t from Ref. 2 (which is also D_t near 180°). Also shown are the predictions of the three most favored phase-shift solutions, Yale 3M and 4M and Arndt and MacGregor solution (Refs. 7, 10, 11).

and low-beam intensity values of D_t. At 25°, because there is no low-intensity data, a value of σ_b equal to the full average difference is used. The error σ_c allows for the uncertainty in the empirical and computed corrections, c_1 and c_2.

The total error in $\bar{D}_t$ is thus due to σ_r, σ_a, σ_b, and σ_c. An "effective" error is obtained by combining them in quadrature. $\bar{D}_t$, its effective error, σ_r, σ_a, σ_b, and σ_c are listed in Table IV. The systematic errors σ_a and σ_b are comparable in importance to the random error.

IV. DISCUSSION

Values of D_t obtained from p-d scattering can be related to the free n-p scattering amplitudes by means of an impulse approximation calculation, as discussed in Refs. 1 and 2. The calculation includes the s-wave final-state interaction between the incident proton and the proton in the deuteron and yields the results:

$$D_t^{pd}=\frac{aI_0^{np}D_t^{np}+2bI_0^{s}D_t^{s}}{aI_0^{np}+2bI_0^{s}}. \quad (9)$$

I_0^{np}, D_t^{np} are the free np cross section and D_t parameters. I_0^s and D_t^s are similar quantities subject to the constraints that the initial neutron-target proton spin state is triplet and the final two-proton spin state is singlet. As D_t^s and D_t^{np} differ only very slightly, D_t^{pd} and D_t^{np} similarly are nearly equal. In Table V are listed the relative amounts of D_t^{np} and D_t^s, $aI_0^{np}/2bI_0^s$; the difference $D_t^{np}-D_t^{pd}$, ΔD; the equivalent free np center-of-mass scattering angles, $\theta_{c.m.}$; and the values of D_t^{np} obtained by adding ΔD to the measurements given in Table IV.

The measured values of D_t^{pd} are plotted in Fig. 3. Also plotted is a point near 0° lab, obtained during an experiment[2] measuring R_t. Note that as $\theta_2\rightarrow 0°$, $R_t\rightarrow D_t$. Curves from the preferred Yale phase shift[7,10] solutions YLAN-3M and 4M, and a recent Livermore[11] energy-independent solution (A-M) are also shown. 3M is for an energy of 210 MeV, while 4M and A-M are for 203 MeV. The differences between these energies and the 197 MeV of the measurements are believed negligible. It is seen that 3M and 4M fit the data quite well, while A-M fits very poorly. This is shown more quantitatively in Table VI, where the χ^2 for the fit by all Yale phase shift sets and the Livermore set are listed.

ACKNOWLEDGMENTS

We wish to thank Dr. R. Wright and Professor G. Breit and Professor P. Signell for helpful communications concerning phase-shift analyses. We are grateful to Professor Alan Cromer for discussions about our impulse-approximation calculation, and for numerical evaluations of the needed coefficients. Computations of P. F. M. Koehler aided in making predictions from the various sets of phase shifts. The experiment depended heavily upon the various support groups of the 130-in. Cyclotron Laboratory: Cyclotron operating crew, mechanical design group, machine shop, and electronics shop.

[10] G. Breit, R. E. Seamon, and R. D. Haracz (private communication).

[11] Richard A. Arndt and Malcolm MacGregor, Phys. Rev. **141**, 873 (1966).